Journal of Solid and Fluid Mechanics (JSFM), 14(2): 1-4, 2024

Shahrood University of Technology

Journal of Solid and Fluid Mechanics (JSFM)

DOI: 10.22044/JSFM.2024.13467.3776

Manufacturing Engineering of Iran

Experimental determination of the parameters of ductile damage model of aluminum 5083 and numerical application of the calibrated model

S. Rasaee[1,*], D. Almasi[2], M. R. Heidari[3]

[1] Asst. Prof., Mech. Eng., Kermanshah university of Technology., Kermanshah, Iran
[2] Adjunct. Prof., Mech. Eng., Kermanshah university of Technology., Kermanshah, Iran
[3] M.Sc. Student, Mech. Eng., Kermanshah university of Technology., Kermanshah, Iran

*Corresponding author: rasaee@kut.ac.ir

Received: 08/20/2023 Revised: 03/18/2024 Accepted: 06/15/2024

Abstract

This study investigates the mechanical behavior and ductile damage phenomena of the Al5083 alloy. The relationship between the fracture strain and the state of stress at the damage location is presented based on the classic damage models of Johnson-Cook, Rice-Tracy, and Hooputra. The results indicate that within the studied stress triaxiality range, the differences between the models are negligible, and each can be utilized with reasonable accuracy. The models were calibrated using experimental results obtained from both smooth and notched flat specimens. To validate the developed model, the deformation process was simulated in Abaqus, and the numerical results were compared to the experimental data. The numerical and experimental simulations showed good agreement, and the extracted model was able to predict the maximum force with an accuracy of ±2.5%.

Keywords: Aluminum 5083, ductile Damage, Johnson-Cook Model, FEM analysis.

1. Introduction

Fracture mechanics methods focus on the local behavior of crack growth and are primarily suited for the analysis of parts with existing cracks. However, they are not well-suited for large-scale rupture analysis of structures. In contrast, damage mechanics, can provide an approximate model of failure that is applicable to the scale of large structures. By employing numerical analysis based on damage mechanics methods, it is possible to predict the potential for defect creation and identify critical locations for the initiation of rupture. Furthermore, this approach allows for the determination of the underlying causes for the formation of such defects.

Numerous behavioral models have been proposed to characterize the response of materials under diverse loading conditions. Developing new models or refining existing ones is necessary to enable the design process and accurately determine material behavior at high strain rates and varying temperatures. The Johnson-Cook model has been extensively utilized due to the relative ease of calibrating the model and determining its associated constants with a limited number of tests. This model is commonly included as a default option in most commercial finite element software, such as Abaqus, for modeling material behavior.

Aviral et al. [1] proposed a method utilizing the Levenberg-Marquardt search algorithm to inversely identify the Johnson-Cook parameters for various materials. The failure of ductile solids is frequently attributed to the growth and coalescence of microscopic voids. In this context, Rice and Tracy [2] investigated the growth of voids under hydrostatic loading and derived a simple exponential relationship for the failure strain in terms of the triaxial stress state. Building upon theoretical and experimental studies, Bai et al. [3, 4] demonstrated that the stress triaxiality is a key parameter in controlling the range of the fracture strain. These findings underscore the importance of accurately characterizing the influence of the stress state on the ductile failure mechanisms of engineering materials.

This research focused on the calibration of the Johnson-Cook damage model for the 5083 aluminum alloy using standard experimental tests. The effectiveness of this model in simulating the rupture of standard samples has been validated. In addition to the standard Johnson-Cook model, the material constants pertaining to the renowned Rice-Tracy and Hooputra models were also extracted. The predictive capabilities of these alternative models were then compared to the Johnson-Cook standard model. The experimental tests were simulated using the Abaqus finite element software, and the resulting force-displacement diagrams were compared to the experimental data. This approach enabled the evaluation of the accuracy and efficiency of the calibrated constitutive models. The findings of this research contribute to the understanding

of the applicability and limitations of various ductile damage models in characterizing the failure behavior of the 5083 aluminum alloy. The insights gained can inform the selection and implementation of appropriate material models for the design and analysis of engineering structures and components.

2. Material Modeling

In metal forming processes, the ductile fracture behavior is influenced by the tolerable strain capacity of the material. Damage will occur if the strain within the material reaches the failure strain. The strain state in the material depends on various parameters, including the prevailing stress conditions. The stress triaxiality parameter is commonly used to quantify the stress state and its influence on the deformation and failure behavior. This parameter captures the ratio of the hydrostatic stress to the von Mises effective stress, providing a measure of the triaxial stress state experienced by the material during the forming operation. Understanding the relationship between the stress triaxiality, material strain, and the onset of ductile fracture is crucial for the reliable design and optimization of metal forming processes. Accurate characterization of this relationship enables the prediction of failure initiation and the implementation of appropriate measures to enhance the formability of the material.

By determining the value of the damage parameter (D), and if the critical damage parameter is known for the material, it is possible to predict the location of crack occurrence as well as the potential sites for rupture initiation. The damage parameter is calculated using the failure strain function in terms of the stress triaxiality parameter (η) and the Load parameter ($\bar{\theta}$) from the following equation:

$$D = \int \frac{d\bar{\varepsilon}_{pl}}{\bar{\varepsilon}_{pl.D}(\eta.\bar{\theta}.\dot{\varepsilon})} \quad (1)$$

In order to use damage mechanics, the relationship between the stress triaxiality parameter and failure strain must first be determined, and the most widely used relationships provided for this issue are Rice-Tracy [2], Johnson-Cook [5] and Hooputra [6] criteria. Based on the Rice-Tracy and Johnson-Cook criteria, the following relationships are used to express the relationship between the stress triaxiality and the failure strain, respectively:

$$\varepsilon_f = c_1 exp(-c_2\eta) \quad (2)$$

$$\varepsilon_f = d_1 + d_2 exp(-d_3\eta) \quad (3)$$

Where c and d are the material constants that are determined from the experiment. In the Hooputra model, according to the following relationship, the plastic failure strain is associated with an exponential function in relation to the stress triaxiality.

$$\varepsilon_f = A\, e^{c\eta} + B\, e^{-c\eta} \quad (4)$$

In this regard, A, B and c are the constants of the material damage criterion and are determined based on experimental tests. These relationships provide the necessary framework to incorporate the effects of the stress state, strain rate, and temperature on the ductile failure behavior of the material within damage mechanics-based approaches.

3. Experimental Procedure

The material characterization was conducted using a standard set of tensile tests according to ASTM E8. Flat grooved specimens with different groove radii (2 mm, 3 mm, 4 mm, and 5 mm) were used to establish the relationship between stress triaxiality and fracture strain (Figure 1). The specimens were cut from a 2×1 meter sheet in three orientations - rolling direction, 45 degrees, and 90 degrees. Each test was repeated three times for statistical significance. The tensile tests were performed using a SANTAM servo-electrical tension device model STM 150, under displacement control at a low speed of 0.01 mm/s. The engineering stress-strain diagrams for the samples in the three orientations are shown in Figure 2, and the true stress-strain behavior of the material is presented in Figure 3, assuming constant volume during plastic deformation. This comprehensive experimental program provided the necessary data to calibrate the constants in the Rice-Tracy and Johnson-Cook failure strain models as a function of the stress triaxiality parameter. To represent the actual plastic stress-strain relationship, an exponential relationship was used, as expressed in the following equation:

$$\sigma = K\varepsilon^n \quad (5)$$

The calculated mechanical properties of the Al5083, are presented in Table 1.

The failure strain was measured using the relationships proposed by Bai et al. [4] for flat samples and Lee et al. [7] for flat-grooved samples and results are presented in Table 2. The constants for the Rice-Tracy, Johnson-Cook, and Hooputra failure criteria were calculated based on the curve fitting, as shown in Table 3. The high correlation coefficients from the curve fitting indicate that the accuracy of the calibrated models is suitable for predicting the ductile failure behavior of the Al5083 under the investigated stress states. The comparison of the results obtained from the different ductile failure models with the experimental data is presented in Figure 5. This comparison reveals that all three models, namely the Rice-Tracy, Johnson-Cook, and Hooputra criteria, exhibit nearly the same predictive capability within the investigated range of stress triaxiality.

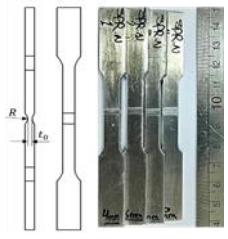

Figure 1. the geometry and prepared Samples for testing

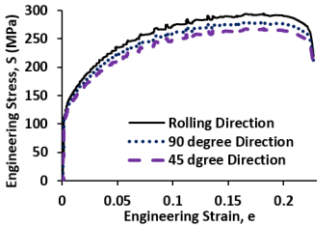

Figure 2. Engineering stress-strain curve of Al5083

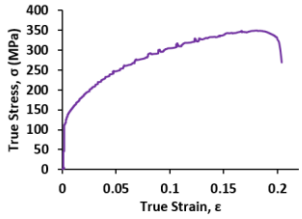

Figure 3. True stress-strain curve of Al5083

Table 1. Mechanical properties of used Al5083

	Mechanical properties
72 GPa	Young's modulus ($\boldsymbol{E}$)
0.33	Poisson's ratio ($\boldsymbol{\vartheta}$)
108 MPa	Yield Stress
541 MPa	strain hardening coefficient ($\boldsymbol{K}$)
0.26	strain-hardening exponent ($\boldsymbol{n}$)

Table 2. Dimensional characteristics and test results of plain and grooved flat samples

Sample Number	Notch Radius (mm)	Thickness (mm)	t_d (mm)	t_f (mm)	Width (mm)
SP.N 0	-	1.98	1.98	1.68	6.21
SPR.N 1	2	1.98	0.99	0.93	6.18
SPR.N 2	3	1.98	1.18	0.99	6.25
SPR.N 3	4	1.98	1.33	1.16	6.17
SPR.N 4	5	1.98	1.23	1.08	6.3

Table 3. Details of damage models, extracted material constants

Rice-Tracey Damage Model: $\boldsymbol{\varepsilon_f = ae^{b\eta}}$			
a	B	Correlation coefficient	
1.246	-3.165	0.93	
Johnson-Cook Damage Model: $\boldsymbol{\varepsilon_f = ae^{b\eta} - c}$			
a	b	C	Correlation coefficient
18.66	0.046-	17.94	0.96
Hooputra Damage Model: $\boldsymbol{\varepsilon_f = ae^{c\eta} + be^{-c\eta}}$			
a	b	C	Correlation coefficient
-1.793	2.511	0.198	0.95

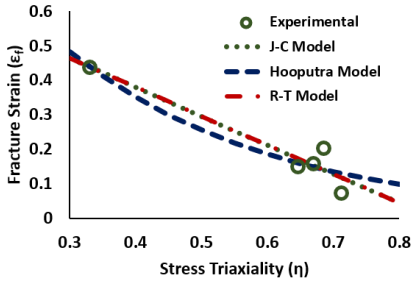

Figure 5. Results of experimental tests and curves obtained from different theories

4. Numerical simulation

Since the models have shown very similar results, also the Johnson-Cook damage model is available by default in Abaqus finite element software, so this model has been used in the simulations. The mechanical properties of the used aluminum alloy according to Table 1 and the non-linear behavior of the material during plastic deformation are considered based on its true stress-strain diagram and as shown in Figure 4.

In the process of simulating the progressive damage, when the damage parameter in each element reaches the critical value, that element is removed. In this study, the displacement parameter at the failure is used as the critical damage parameter, and 0.03mm has been determined for it. The entire geometry is modeled, and the model is meshed with C3D8R cubic 8-node elements and an explicit solver is used to analyze the problem. Validation and accuracy of simulation is obtained by comparing the results of simulation with the results of experimental tests. the force-displacement response and the displacement before rupture are considered as parameters to control the accuracy.

Figure 6a shows the experimental and numerical force-displacement diagram for the flat sample. The convergence diagrams show that the modeling with 4,896 elements has been able to predict the maximum force with very high accuracy (error less than 1%), although it is less accurate in predicting the displacement at rupture (an error of about 8.6%).

In Figure 6b, the results of considering the damage model, along with the comparison of the appearance of experimental and simulated samples, are shown. The effect of applying the damage model on the simulation has been significant. When the damage criterion is not included, the force-displacement diagram has no limitations. Also, as is clear from the figure, the location and pattern of failure are completely consistent with the experimental sample.

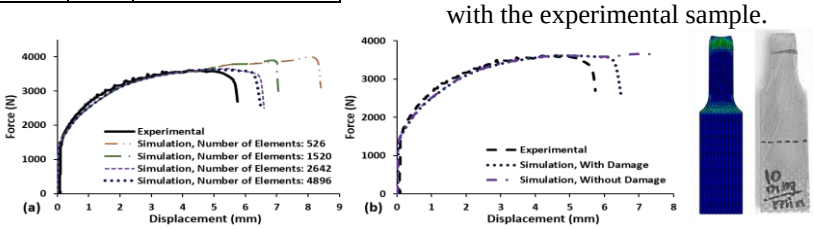

Figure 6. Results of experimental tests and curves obtained from failure equations for SP.N0 sample

In general, the presented numerical model has been able to calculate the maximum force values with better accuracy, but the determination of the displacement at failure has been significantly less accurate. Examining the results shows that the error percentage of the predicted maximum force is less than 0.1%, whereas the error related to the displacement of the sample at the moment of loss of load-bearing capacity is around 8.6%. The cause of this discrepancy in predicting the displacement at failure can be attributed to the difference between the plane stress state of the experimental tensile samples and the relationships used to calculate the fracture strain and stress triaxiality, which are typically derived for the plane strain condition.

Flat grooved samples that have transverse grooves are known as plane strain samples, and the criteria and equations presented in this research are also derived based on these samples. The plane strain mode is the most conservative mode at the beginning of the damage process, while the samples used for the experiments were done with low width, which is close to a plane stress state.

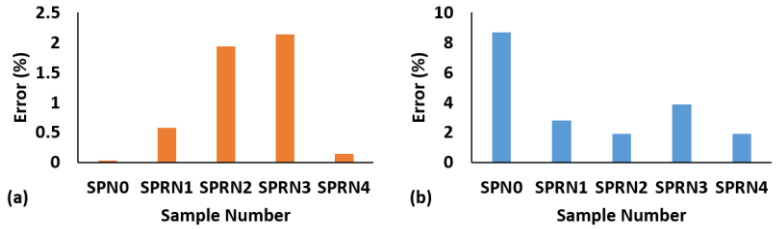

Figure 7. Calculated error in determining the value of a) maximum force, b) displacement at failure

Based on the obtained results, the errors are presented in the form of diagrams in Figure 7. In general, the calibrated model was able to better predict the maximum force value for samples without grooves, but in grooved samples, the accuracy of predicting the value of fracture displacement was better. The cause of this problem may be the creation of a state of stress triaxiality due to the presence of the groove and the effect of the hydrostatic stress components on limiting the deformation around the groove. According to the obtained results and acceptable errors, it can be concluded that the methods presented in this research have an acceptable agreement with the experimental results to investigate the damage phenomenon in engineering analyses for aluminum 5083, and these relationships can be used to determine the damage and breakage. These methods can also be used in forming processes with complex geometry.

5. Conclusion

The ductile damage model of the 5083 aluminum alloy based on standard models, where is assumed fracture strain as a function of stress triaxiality parameter, calibrated. To validate the efficiency of the model, the tests have also been simulated in Abaqus. The study of the accuracy of the results shows that although the presented models are quite accurate in predicting the maximum force and have predicted it with an error of less than 2.5%, they are less accurate for calculating the amount of displacement until the onset of failure, and in the worst case, the accuracy is less than 8%. It is necessary to pay attention to the fact that the models used are presented for plane strain conditions, and the tests performed to extract the material constants were in a state of plane stress. This point can be considered as one of the causes of the error. Also, for the specimen without a groove, the damage criterion has been predicted earlier, and the reason can be the conservative state of plane strain.

6. References

[1] Shrot, A. and M. Bäker, Determination of Johnson–Cook parameters from machining simulations. *Computational Materials Science*, 2012. 52(1): p. 298-304.

[2] Rice, J.R. and D.M. Tracey, On the ductile enlargement of voids in triaxial stress fields∗. *Journal of the Mechanics and Physics of Solids*, 1969. 17(3): p. 201-217.

[3] Bai, Y., X. Teng, and T. Wierzbicki, On the Application of Stress Triaxiality Formula for Plane Strain Fracture Testing. *Journal of Engineering Materials and Technology*, 2009. 131(2).

[4] Bai, Y. and T. Wierzbicki, A new model of metal plasticity and fracture with pressure and Lode dependence. *International Journal of Plasticity*, 2008. 24(6): p. 1071-1096.

[5] Johnson, G.R. and W.H. Cook, Fracture characteristics of three metals subjected to various strains, strain rates, temperatures and pressures. *Engineering Fracture Mechanics*, 1985. 21(1): p. 31-48.

[6] Hooputra, H., et al., A comprehensive failure model for crashworthiness simulation of aluminium extrusions. *International Journal of Crashworthiness*, 2004. 9(5): p. 449-464.

[7] Lee, Y.-W., *Fracture prediction in metal sheets*. 2006.